

Absorption Spectra, Photophysical Properties, and Redox Behavior of Stereochemically Pure Dendritic Ruthenium(II) Tetramers and Related Dinuclear and Mononuclear Complexes

Sebastiano Campagna,^{*,†} Scolastica Serroni,[†] Swamy Bodige,[‡] and Frederick M. MacDonnell^{*,‡}

Dipartimento di Chimica Inorganica, Chimica Analitica e Chimica Fisica, Università di Messina, Via Sperone 31, 98166, Messina, Italy, and Department of Chemistry and Biochemistry, University of Texas at Arlington, Arlington, Texas 76019

Received October 6, 1998

The absorption spectra, luminescence properties, and redox behavior of stereochemically pure, dendritic Ru(II) tetramers have been studied. Furthermore, the investigation has also been performed on stereochemically resolved dinuclear complexes of the same family and on racemic forms of their mononuclear precursors and models. The complexes studied are the racemic species [(phen)₂Ru(1,10-phenanthroline-5,6-dione)](PF₆)₂ (**A**, phen = 1,10-phenanthroline), [(phen)₂Ru(1,10-phenanthroline-5,6-diamine)](PF₆)₂ (**B**), [Ru(1,10-phenanthroline-5,6-dione)₃](PF₆)₂ (**C**), [(phen)₂Ru(tpphz)](PF₆)₂ (**1**, tpphz = tetrapyrido[3,2-*a*:2',3'-*c*:3'',2''-*h*:2'',3''-*j*]phenazine), [(phen)₂Ru(μ-tpphz)Ru(phen)₂](PF₆)₄ (**2**), and [{(phen)₂Ru(μ-tpphz)}₃Ru](PF₆)₈ (**4**), the stereochemically pure dinuclear species ΔΔ-[(phen)₂Ru(μ-tpphz)Ru(phen)₂](PF₆)₄ (ΔΔ-**2**), ΛΛ-[(phen)₂Ru(μ-tpphz)Ru(phen)₂](PF₆)₄ (ΛΛ-**2**), and ΔΛ-[(phen)₂Ru(μ-tpphz)Ru(phen)₂](PF₆)₄ (ΔΛ-**2**), and the stereochemically pure dendritic tetranuclear complexes [(Δ-(phen)₂Ru(μ-tpphz))₃-Δ-Ru](PF₆)₈ (Δ₃Δ-**4**), [(Δ-(phen)₂Ru(μ-tpphz))₃-Λ-Ru](PF₆)₈ (Δ₃Λ-**4**), and [(Λ-(phen)₂Ru(μ-tpphz))₃-Λ-Ru](PF₆)₈ (Λ₃Λ-**4**). All the complexes exhibit reversible metal-centered oxidation processes: the mononuclear complexes undergo a one-electron oxidation within the potential range +1.30 to +1.70 V vs SCE, whereas the dinuclear complexes undergo a two-electron oxidation at about +1.35 V and the tetranuclear compounds undergo a three-electron process at about +1.35 V followed by a one-electron process at +1.46 V. On reduction, each compound undergoes several reversible or quasireversible ligand-centered reductions within the potential window investigated (+2.00/−1.80 V vs SCE). The absorption spectra of the complexes exhibit intense ligand-centered (LC) bands in the UV region (ε up to 10⁶ M^{−1} cm^{−1}) and moderately intense metal-to-ligand charge-transfer (MLCT) bands in the visible region (ε in the range 10⁴–10⁵ M^{−1} cm^{−1}). All the complexes are luminescent both in fluid acetonitrile solution at room temperature (λ_{max} in the range 600–720 nm) and in MeOH/EtOH 4:1 (v/v) rigid matrix at 77 K (λ_{max} in the range 560–620 nm), except **C** which is luminescent only at 77 K. In all the cases, luminescence decays are monoexponential with lifetimes in the range 10^{−5}–10^{−8} s. Energy transfer occurs in the dendritic tetranuclear complexes from the central chromophore to the peripheral ones. For the oligonuclear tpphz-containing complexes, luminescence at room temperature and at 77 K originates from different MLCT states. When the experimental uncertainties are taken into account, the absorption spectra, luminescence properties, and redox behavior of the various stereoisomers studied here are practically undistinguishable one another. Comparison of our results with the photophysical results reported for other stereochemically pure luminescent multimetallic arrays is attempted.

Introduction

Luminescent and redox-active oligonuclear polypyridine metal complexes with controlled topologies are extensively studied because they are quite attractive for several theoretical and applicative purposes.¹ For example, they can be used as components to assembly large and functional arrays (supramolecular species) for light-energy conversion processes² and information storage.³ In particular, luminescent dendrimers made

of Ru(II) and/or Os(II)-polypyridine building blocks are the object of increasing investigations,^{4–6} because such structures can be used to spatially and configurationally organize these

[†] Università di Messina.

[‡] University of Texas at Arlington.

(1) (a) Balzani, V.; Scandola, F. *Supramolecular Photochemistry*; Ellis Horwood: Chichester, 1991. (b) Kalyanasundaram, K. *Photochemistry of Polypyridine and Porphyrin Complexes*; Academic Press: London, 1992. (c) Lehn, J.-M. *Supramolecular Chemistry*; VCH: Weinheim, 1995. (d) Balzani, V.; Juris, A.; Venturi, M.; Campagna, S.; Serroni, S. *Chem. Rev.* **1996**, *96*, 759 and references therein. (e) Collin, J.-P.; Gaviña, P.; Heitz, V.; Sauvage, J.-P. *Eur. J. Inorg. Chem.* **1998**, *1*,

(2) (a) Meyer, T. *J. Acc. Chem. Res.* **1989**, *22*, 163. (b) Molnar, S. M.; Nallas, G.; Bridgewater, J. S.; Brewer, K. J. *J. Am. Chem. Soc.* **1994**, *116*, 5206. (c) Hagfeldt, A.; Graetzel, M. *Chem. Rev.* **1995**, *95*, 49. (d) Grosshenny, V.; Harriman, A.; Ziessel, R. *Angew. Chem., Int. Ed. Engl.* **1995**, *34*, 1100. (e) Shaw, J. R.; Sadler, G. S.; Wacholtz, W. F.; Ryu, C. K.; Schmehl, R. H. *New J. Chem.* **1996**, *20*, 749. (f) Bignozzi, C. A.; Schoonover, J. R.; Scandola, F. *Prog. Inorg. Chem.* **1997**, *44*, 1. (g) Balzani, V.; Campagna, S.; Dent, G.; Juris, A.; Serroni, S.; Venturi, M. *Acc. Chem. Res.* **1998**, *31*, 26. (3) (a) Balzani, V.; Credi, A.; Scandola, F. In *Transition Metals in Supramolecular Chemistry*; Fabbrizzi, L., Poggi, A., Eds.; Kluwer: Dordrecht, The Netherlands, 1994; p 1. (b) Hanan, G. S.; Arana, C. R.; Lehn, J.-M.; Baum, G.; Fenske, D. *Chem. Eur. J.* **1996**, *2*, 1292. (c) Collin, J.-P.; Gaviña, P.; Sauvage, J.-P. *New J. Chem.* **1997**, *21*, 525. (d) Balzani, V.; Credi, A.; Venturi, M. *Curr. Opin. Chem. Biol.* **1997**, *1*, 506.

building blocks in a manner which is well suited to take full advantage of their electrochemical, photophysical, and stereochemical properties. However, relatively little attention has been paid to the absolute stereochemistry of these supermolecules, due to difficulties in efficient stereospecific synthesis of chiral metal-based dendrimers with bidentate polypyridine ligands.

Recently, some of us^{7,8} as well as other^{9–11} research groups have developed strategies to assemble enantiomerically pure luminescent polynuclear metal complexes, and photophysical studies of pure polynuclear Ru(II) stereoisomers have started to appear.^{11a,12,13} Here we report the first investigation on the absorption spectra, photophysical and redox properties of the series of enantiomerically and diastereomerically pure tetranuclear dendrimers having Ru(II) centers as branching sites. The complexes studied are $[(\Delta-(\text{phen})_2\text{Ru}(\mu\text{-tpphz}))_3-\Delta\text{-Ru}](\text{PF}_6)_8$ ($\Delta_3\Delta\text{-4}$; phen = 1,10-phenanthroline and tpphz = tetrapyrido[3,2-*a*:2',3'-*c*:3'',2''-*h*:2''',3''-*j*]phenazine), $[(\Delta-(\text{phen})_2\text{Ru}(\mu\text{-tpphz}))_3-\Lambda\text{-Ru}](\text{PF}_6)_8$ ($\Delta_3\Lambda\text{-4}$), $[(\Lambda-(\text{phen})_2\text{Ru}(\mu\text{-tpphz}))_3-\Lambda\text{-Ru}](\text{PF}_6)_8$ ($\Lambda_3\Lambda\text{-4}$), and a statistical mixture of all eight isomeric forms prepared from racemic starting materials, denoted mix-4. The properties of all the three possible enantiomerically pure dinuclear species $\Delta\Delta$ - $[(\text{phen})_2\text{Ru}(\mu\text{-tpphz})\text{Ru}(\text{phen})_2](\text{PF}_6)_4$ ($\Delta\Delta\text{-2}$), $\Lambda\Lambda$ - $[(\text{phen})_2\text{Ru}(\mu\text{-tpphz})\text{Ru}(\text{phen})_2](\text{PF}_6)_4$ ($\Lambda\Lambda\text{-2}$), and $\Delta\Lambda$ - $[(\text{phen})_2\text{Ru}(\mu\text{-tpphz})\text{Ru}(\text{phen})_2](\text{PF}_6)_4$ ($\Delta\Lambda\text{-2}$) and their isomeric mixture, mix-2, which can be considered as low-nuclearity analogues of the tetranuclear dendrimers, together with the properties of the mononuclear precursors $[(\text{phen})_2\text{Ru}(\text{phendione})](\text{PF}_6)_2$ (**A**; phendione = 1,10-phenanthroline-5,6-dione), $[(\text{phen})_2\text{-}$

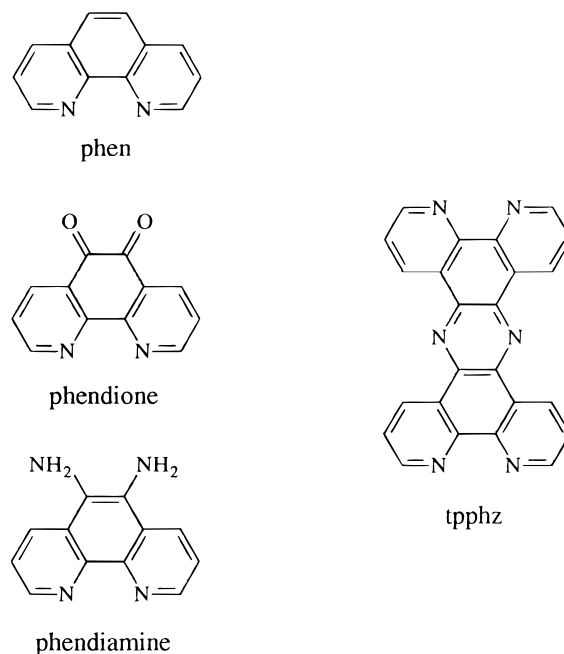


Figure 1. Structural formulas of the ligands.

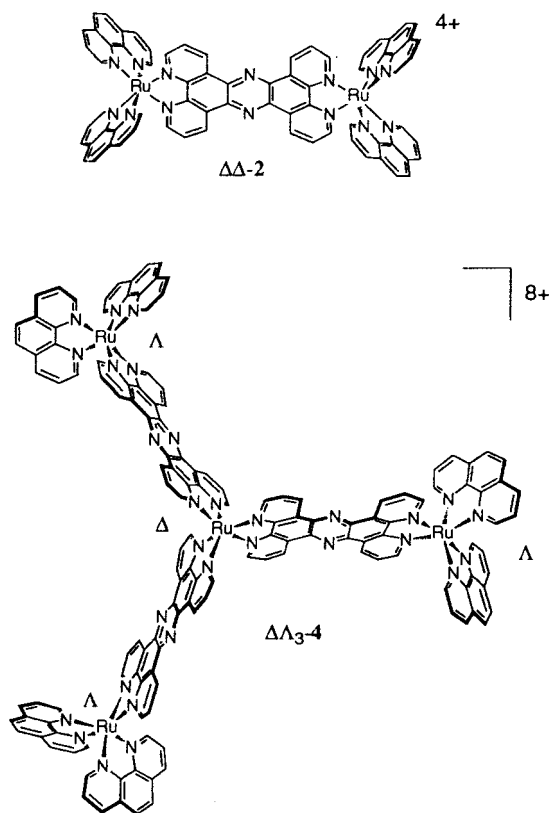


Figure 2. Schematic representation of selected dinuclear and dendritic tetranuclear complexes.

Ru(phendiamine)](PF_6)₂ (**B**; phendiamine = 1,10-phenanthroline-5,6-diamine), and $[\text{Ru}(\text{phendione})_3](\text{PF}_6)_2$ (**C**), and of the model compound $[(\text{phen})_2\text{Ru}(\text{tpphz})](\text{PF}_6)_2$ (**1**) are also reported. The structural formulas of the polypyridine ligands are shown in Figure 1, and the schematic representations of $\Delta\Delta\text{-2}$ and $\Delta\Lambda_3\text{-4}$ are shown in Figure 2.

Experimental Section

Materials and Methods. The synthesis of all the complexes studied have been reported elsewhere.^{7,8} Ab initio calculations were performed

- (4) (a) Denti, G.; Campagna, S.; Serroni, S.; Ciano, M.; Balzani, V. *J. Am. Chem. Soc.* **1992**, *114*, 2944. (b) Serroni, S.; Juris, A.; Campagna, S.; Venturi, M.; Denti, G.; Balzani, V. *J. Am. Chem. Soc.* **1994**, *116*, 9086. (c) Campagna, S.; Denti, G.; Serroni, S.; Juris, A.; Venturi, M.; Ricevuto, V.; Balzani, V. *Chem. Eur. J.* **1995**, *1*, 211. (d) Serroni, S.; Campagna, S.; Denti, G.; Juris, A.; Venturi, M.; Balzani, V. In *Advances in Dendritic Macromolecules*; Newkome, G. R., Ed.; JAI Press: London, 1996; Vol. 3, p 115. (e) Serroni, S.; Juris, A.; Venturi, M.; Campagna, S.; Resino, I. R.; Denti, G.; Credi, A.; Balzani, V. *J. Mater. Chem.* **1997**, *7*, 1227. (f) Venturi, M.; Serroni, S.; Juris, A.; Campagna, S.; Balzani, V. *Top. Curr. Chem.* **1998**, *197*, 193.
- (5) (a) Murphy, W. R.; Brewer, K. J.; Gettiffe, G.; Petersen, J. D. *Inorg. Chem.* **1989**, *28*, 81. (b) Jacquet, L.; Kirsch-De Mesmaeker, A. *J. Chem. Soc., Faraday Trans.* **1992**, *88*, 2471. (c) Haga, M.; Ali, M. M.; Arakawa, R. *Angew. Chem., Int. Ed. Engl.* **1996**, *35*, 76. (d) Moucheron, C.; Kirsch-De Mesmaeker, A.; Dupont-Gervais, A.; Leize, E.; Van Dorsselaer, A. *J. Am. Chem. Soc.* **1996**, *118*, 12834. (e) Issberner, J.; Vögtle, F.; De Cola, L.; Balzani, V. *Chem. Eur. J.* **1997**, *3*, 706.
- (6) (a) Newkome, G. R.; Cardullo, F.; Constable, E. C.; Moorefield, C. N.; Cargill Thompson, A. M. W. *J. Chem. Soc. Chem. Commun.* **1993**, 925. (b) Constable, E. C.; Harveson, P. *Chem. Commun.* **1996**, 33. (c) Constable, E. C.; Harveson, P.; Oberholzer, M. *Chem. Commun.* **1996**, 1821. (d) Constable, E. C. *Chem. Commun.* **1997**, 1073 and references therein.
- (7) (a) MacDonnell, F. M.; Bodige, S. *Inorg. Chem.* **1996**, *35*, 2601. (b) Bodige, S.; MacDonnell, F. M. *Tetrahedron Lett.* **1997**, *38*, 8159.
- (8) Bodige, S.; Torres, A. S.; Maloney, D. J.; Tate, D.; Kinsel, G.; Walker, A.; MacDonnell, F. M. *J. Am. Chem. Soc.* **1997**, *119*, 10364.
- (9) (a) Hua, X.; von Zelewsky, A. *Inorg. Chem.* **1991**, *30*, 3796. (b) Hayoz, P.; von Zelewsky, A.; Stoekli-Evans, H. *J. Am. Chem. Soc.* **1993**, *115*, 5111. (c) Hua, X.; von Zelewsky, A. *Inorg. Chem.* **1995**, *34*, 5791.
- (10) (a) Rutherford, T. J.; Quagliotto, M. G.; Keene, F. R. *Inorg. Chem.* **1995**, *34*, 3857. (b) Rutherford, T. J.; Keene, F. R. *Inorg. Chem.* **1997**, *36*, 3580. (c) Morgan, O.; Wang, S.; Bae, S.-A.; Morgan, R. J.; Baker, A. D.; Streckas, T. C.; Engel, R. *J. Chem. Soc., Dalton Trans.* **1997**, 3773. (d) Tzalis, D.; Tor, Y. *J. Am. Chem. Soc.* **1997**, *119*, 852. (e) Patterson, B. T.; Keene, F. R. *Inorg. Chem.* **1998**, *37*, 645.
- (11) (a) Warnmark, K.; Thomas, J. A.; Heyke, O.; Lehn, J.-M. *Chem. Commun.* **1996**, 701. (b) Warnmark, K.; Heyke, O.; Thomas, J. A.; Lehn, J.-M. *Chem. Commun.* **1996**, 2603.
- (12) Rutherford, T. J.; Van Gijte, O.; Kirsch-De Mesmaeker, A.; Keene, F. R. *Inorg. Chem.* **1997**, *36*, 4465.
- (13) Fletcher, N. C.; Keene, F. R.; Viebrock, H.; von Zelewsky, A. *Inorg. Chem.* **1997**, *36*, 4465.

Table 1. Absorption and Luminescence Properties in Acetonitrile-Deaerated Solution, Unless Otherwise Noted

	absorption 298 K		luminescence			
	λ_{\max} , nm (ϵ , M ⁻¹ cm ⁻¹) ^b	298 K		77 K ^a		
		λ_{\max} , nm	τ , ns	Φ	λ_{\max} , nm	τ , μ s
Mononuclear Complexes						
[Ru(phen) ₃] ²⁺ ^c	442 (18000)	604	460	2.8×10^{-2}	565	10.0
A [(phen) ₂ Ru(phenidione)] ²⁺	434 (14800)	625	5	9.6×10^{-4}	600	4.9
B [(phen) ₂ Ru(phenidiamine)] ²⁺	455 sh (15200)	650	1740	1.4×10^{-2}	585	4.7
C [Ru(phenidione) ₃] ²⁺	417 (14700)	no emission			600	4.9
1 [(tpphz)Ru(phen) ₂] ²⁺	445 (18500)	625	1250	7.3×10^{-2}	580	5.9
Dinuclear Complexes						
mix-2 [(phen) ₂ Ru(tpphz)Ru(phen) ₂] ⁴⁺	439 (35900)	710	90	5.0×10^{-3}	583	4.1
$\Delta\Delta$ -2	439 (36500)	710	105	6.0×10^{-3}	584	4.5
$\Lambda\Lambda$ -2	438 (35500)	710	125	5.6×10^{-3}	583	4.4
$\Delta\Delta$ -2	439 (38100)	710	110	5.4×10^{-3}	586	4.4
Tetranuclear Complexes						
mix-4 [Ru{(tpphz)Ru(phen) ₂ }] ₃ ⁸⁺	442 (86000)	715	75	3.0×10^{-3}	594	3.9
$\Delta\Delta_3$ -4	439 (86000)	718	75	3.0×10^{-3}	594	3.9
$\Delta\Lambda_3$ -4	439 (78000)	715	74	2.9×10^{-3}	596	3.6
$\Lambda\Lambda_3$ -4	441 (76000)	720	81	2.0×10^{-3}	596	3.2

^a In MeOH/EtOH 4:1 (v/v). ^b Only the lowest energy maximum or shoulder is given. ^c Data from literature (Kawanishi, Y.; Kitamura, N.; Kim, Y.; Tazuke, S. *Riken Q.* **1984**, 78, 212. Cocks, A. T.; Wright, R. D.; Seddon, K. R. *Chem. Phys. Lett.* **1982**, 85, 369).

using the PC Spartan Plus software package. Absorption spectra have been performed with a Kontron Uvikon 860 spectrophotometer. For luminescence spectra, a Perkin-Elmer LS-5B fluorimeter, equipped with a Hamamatsu R 928 photomultiplier, was used. Luminescence spectra were corrected for photomultiplier response by calibrating the fluorimeter with a standard lamp. Luminescence lifetimes have been obtained by a Edinburgh FL-900 time-correlated single-photon-counting spectrometer using nitrogen discharge as pulsed-light source (pulse width: 3 ns). The emission decay traces were deconvoluted for the instrumental flashlamp by Marquadt algorithm. For each measurement, at least five determinations were carried out. Luminescence quantum yields were calculated by the optically diluted method¹⁴ using [Ru(bpy)₃]²⁺ in aerated water as a reference ($\Phi = 0.028^{15}$). When necessary, samples were deoxygenated by bubbling nitrogen for at least 20 min. Electrochemical measurements were carried out in argon-purged acetonitrile at room temperature with a PAR 273 multipurpose equipment interfaced to a PC. The working electrode was a Pt microelectrode or a glassy carbon (8 mm², Amel) electrode. The counter electrode was a Pt wire, and the reference electrode was a SCE separated with a fine glass frit. The concentration of the complexes was about 5×10^{-4} M. Tetraethylammonium hexafluorophosphate was used as supporting electrolyte and its concentration was 0.05 M. Cyclic voltammograms were obtained at scan rates of 50, 500, and 1000 mV/s. For reversible processes, half-wave potentials (vs SCE) were calculated as an average of the cathodic and anodic peaks. The criteria for reversibility were the separation between cathodic and anodic peaks, the close-to-unity ratio of the intensities of the cathodic and anodic currents, and the constancy of the peak potential on changing scan rate. The number of exchanged electrons was measured with differential pulse voltammetry (DPV) experiments performed with a scan rate of 20 mV/s, a pulse height of 75 mV, and a duration of 40 ms. The procedure for the calibration of the number of electrons corresponding to the various redox waves has been described in detail.^{4,c,e}

Experimental errors in the reported data are as follows: absorption maxima, 2 nm; emission maxima, 4 nm; molar absorption coefficients, 10%; emission lifetimes, 10%; emission quantum yields, 20%; redox potentials, ± 10 mV.

Results

All the complexes studied are stable in the solvents used, as demonstrated by the constancy of their absorption spectra within 1 week.

All the complexes exhibit reversible metal-centered oxidation processes. The mononuclear complexes undergo a one-electron oxidation within the potential range +1.30 to +1.70 V vs SCE, whereas the dinuclear complexes undergo a two-electron oxidation at +1.35 V and the tetranuclear dendritic compounds undergo a three-electron process at +1.35 followed by a one-electron process at +1.45 V. On reduction, each compounds undergo several reversible or quasi-reversible ligand-centered reductions within the potential window investigated (+2.00/−1.80 V vs SCE).

The absorption spectra of the complexes exhibit intense bands in the UV region (ϵ up to 10^6 M⁻¹ cm⁻¹) and moderately intense bands in the visible region (ϵ in the range 10^4 – 10^5 M⁻¹ cm⁻¹). All the complexes are luminescent both in fluid acetonitrile solution at room temperature (λ_{\max} in the range 600–720 nm) and in MeOH/EtOH 4:1 (v/v) rigid matrix at 77 K (λ_{\max} in the range 560–620 nm), except **C** which is luminescent only at 77 K in a rigid matrix. In all the cases, luminescence decays are monoexponential and luminescence spectra are independent of excitation wavelength. At 77 K, all the luminescence spectra exhibit a vibrational progression of about 1300 cm⁻¹. Excitation spectra were performed for all the luminescent complexes in fluid solution (emission collected in their own emission maxima) and they were found to closely match the relative absorption spectra.

Absorption and luminescence data are gathered in Table 1. Table 2 collects the redox properties of the complexes. Figure 3 shows absorption and 77 K luminescence spectra of **A**, **B**, and **C**; Figures 4 and 5 show absorption and luminescence spectra of **1**, $\Delta\Delta$ -2, and $\Delta\Lambda_3$ -4.

Discussion

The spectroscopic and electrochemical properties of transition metal complexes are usually discussed with the assumption that the ground state as well as the excited and redox states involved can be described by a localized molecular orbital configuration.^{16,17} Within such an assumption, the various spectroscopic

(14) Demas, J. N.; Crosby, G. A. *J. Phys. Chem.* **1971**, 75, 991.

(15) Nakamaru, K. *Bull. Chem. Soc. Jpn.* **1982**, 55, 2697.

(16) Balzani, V.; Carassiti, V. *Photochemistry of Coordination Compounds*; Academic: London, 1970.

(17) Juris, A.; Balzani, V.; Barigelletti, F.; Campagna, S.; Belser, P.; von Zelewsky, A. *Coord. Chem. Rev.* **1988**, 84, 85.

Table 2. Redox Potentials in Argon-Purged Acetonitrile Solution, 298 K

compound	$E_{1/2}^{\text{red}} (n)^a$					$E_{1/2}^{\text{ox}} (n)^a$	
	phendione	phendione	tpphz	phen	phen	Ru	
[Ru(phen) ₃] ²⁺ ^b				-1.35 (1)	-1.52 (1)	+1.27 (1)	
A [(phen) ₂ Ru(phendione)] ²⁺	-0.51 (1)	-0.81 (1)		-1.43 (1)	-1.73 ^c	+1.41 (1)	
B [(phen) ₂ Ru(phendiamine)] ²⁺				-1.35 (1)		+1.31 (1)	
C [Ru(phendione) ₃] ²⁺			adsorption			+1.64 (1)	
1 [(phen) ₂ Ru(tpphz)] ²⁺			-1.00 (1)	-1.38 (1)	-1.69 (1)	+1.34 (1)	
mix-2 [(phen) ₂ Ru(tpphz)Ru(phen) ₂] ⁴⁺			-0.78 (1)	-1.36 (2)	-1.52 ^c	+1.34 (2)	
ΔΔ-2			-0.78 (1)	-1.35 (2)	-1.56 ^c	+1.35 (2)	
ΛΛ-2			-0.78 (1)	-1.36 (2)	-1.55 ^c	+1.35 (2)	
ΔΛ-2			-0.78 (1)	-1.36 (2)	-1.55 ^c	+1.34 (2)	
mix-4 [Ru{(tpphz)Ru(phen) ₂ }] ₃ ¹⁸⁺			-0.78 (3)	-1.35 (3)	-1.54 ^c	+1.35 (3) ^d	+1.46 (1) ^e
ΔΔ ₃ -4			-0.79 (3)	-1.36 (3)	-1.55 ^c	+1.36 (3) ^d	+1.47 (1) ^e
ΔΛ ₃ -4			-0.78 (3)	-1.36 (3)	-1.56 ^c	+1.35 (3) ^d	+1.47 (1) ^e
ΛΔ ₃ -4			-0.79 (3)	-1.35 (3)	-1.52 ^c	+1.36 (3) ^d	+1.46 (1) ^e

^a In parenthesis the number of exchanged electrons is given. ^b Data from: Barigelletti, F.; Juris, A.; Balzani, A.; Belser, P.; von Zelewsky, A. *Inorg. Chem.* **1987**, *26*, 4115. ^c It is not possible to estimate the number of exchanged electrons because of adsorption phenomena. ^d Oxidation of the peripheral metals. ^e Oxidation of the central metal.

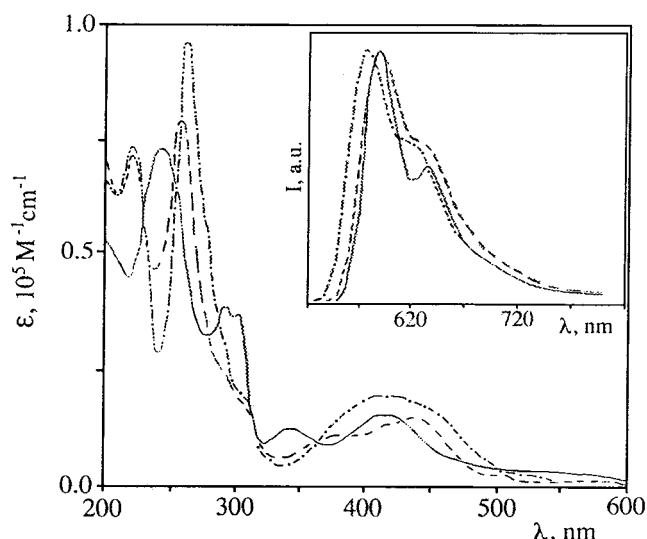


Figure 3. Absorption spectra of **A** (dashed line), **B** (solid line), and **C** (dotted) in acetonitrile solution at room temperature and (inset) luminescence spectra of the same complexes in MeOH/EtOH 4:1 (v/v) rigid matrix at 77 K. Luminescence spectra are uncorrected for photomultiplier response. For corrected data, see Table 1.

transitions are classified as metal-centered (MC), ligand-centered (LC), or charge-transfer (either metal-to-ligand, MLCT, or ligand-to-metal, LMCT), and the oxidation and reduction processes are classified as metal- or ligand-centered.

As a first step in the discussion of the properties of the studied complexes, we will discuss the properties of the mononuclear and mix-2 and mix-4 oligonuclear species. Then, the differences between the stereoisomers will be discussed.

Redox Behavior. Mononuclear Complexes. The one-electron metal-centered oxidation process of all the complexes occurs in a relatively narrow range of potentials (Table 1). The differences in the oxidation potentials can be explained by the effect of the variation in the electron withdrawing ability of the ligands on passing from phen to 1,10-phenanthroline-5,6-diamine (here after, phendiamine), tpphz, and 1,10-phenanthroline-5,6-dione (here after, phendione). Phendiamine has an electron withdrawing ability very similar to phen, so that only slight differences in the metal oxidation potential between [Ru(phen)₃]²⁺ and **B** was noted, whereas tpphz and phendione are better electron-withdrawing ligands and the oxidation of **A**, **C**, and **1** occur at more positive potentials.

The analysis of the reduction patterns was often complicated

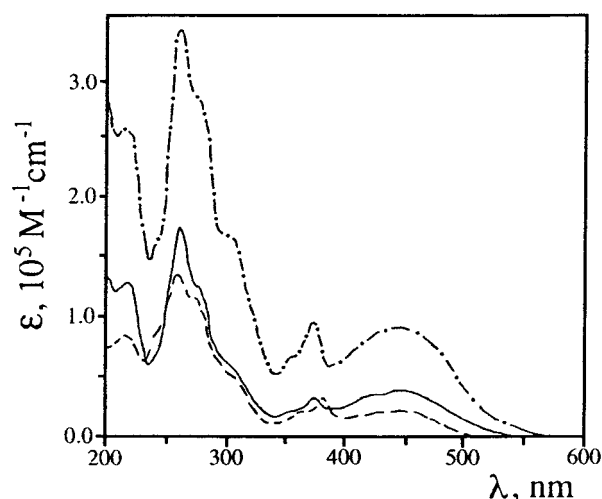


Figure 4. Absorption spectra of **1** (dashed line), ΔΔ-2 (solid line), and ΔΔ-4 (dotted line) in acetonitrile.

by adsorption of the reduced forms of the complexes on the electrodes. However, by careful comparison of the reduction patterns of all the complexes, assignment of each process to a specific ligand in several cases was made (Table 2). It is interesting to note that in **A** the first two processes can be assigned to successive one-electron reduction of the phendione ligand, in that they occur at a significantly less negative potentials than usual phen-based reductions in Ru(II) complexes.¹⁷ Ligands such as phendione are in fact known to undergo a reversible two-electron/two-proton process in protic solvents at less negative potentials.¹⁸ Acetonitrile evidently stabilizes the successive one-electron reductions. As far as **B** is concerned, the first reduction is assigned to a phen ligand (Table 2). At more negative potentials, irreversible processes occur. Reduction processes of **C** could not be studied because of the already cited adsorption problems.

The reduction pattern of **1** is qualitatively similar to that reported^{19,20} for the related complex [(bpy)₂Ru(tpphz)]²⁺ (bpy = 2,2'-bipyridine). To rationalize these results it is useful to observe that two orbitals very close in energy are present in tpphz, LUMO and LUMO+1 as determined by ab initio

(18) Goss, C. A.; Abruna, H. D. *Inorg. Chem.* **1985**, *24*, 4263.

(19) Bolger, J.; Gourdon, A.; Ishow, E.; Launay, J.-P. *J. Chem. Soc., Chem. Commun.* **1995**, 1799.

(20) Bolger, J.; Gourdon, A.; Ishow, E.; Launay, J.-P. *Inorg. Chem.* **1996**, *35*, 2937.

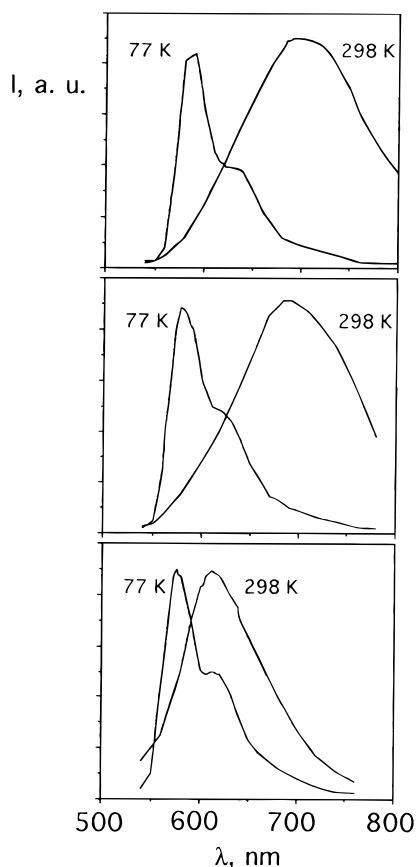


Figure 5. Luminescence spectra (uncorrected) of **1** (bottom), $\Delta\Delta$ -**2** (middle), and $\Delta_3\Delta$ -**4** (top) in acetonitrile at room temperature and in MeOH/EtOH 4:1 (v/v) rigid matrix at 77 K. In each case, the 77 K emission spectrum is the one peaking at higher energy.

calculations (3-21G basis set) on free tpphz. These calculations agree qualitatively with those previously obtained via the extended-Hückel method.²⁰ As can be seen in Figure 6, the LUMO is mainly centered on the pyrazine portion of the bridge, receiving negligible contribution from the phenanthroline nitrogens, whereas the LUMO+1 is mainly centered on the phenanthroline subunits, receiving negligible contribution from the pyrazine nitrogens. In fact, the similarity of the phenanthroline LUMO and the LUMO+1 on tpphz is obvious as can be seen in Figure 6, except that the tpphz LUMO+1 is 0.78 eV lower in energy. Metal coordination modifies the situation, but not in a qualitative way. So the first reduction of **1** is assigned to the LUMO, localized at the pyrazine site. While the LUMO+1 of tpphz is lower in energy than the LUMO orbital of phen, the presence of one additional electron on the pyrazine site of tpphz is expected to raise its energy, so that second and third reductions should involve the phenanthroline ligands.

Oligonuclear Complexes. In “symmetric” dinuclear polypyridine complexes, the pattern of metal oxidation is connected to the electronic interaction between the metals mediated by the bridging ligands.^{21,22} When electronic communication between metals is large, two successive metal-centered one-electron oxidations occur, whereas when the metal–metal interaction is relatively small, two one-electron processes occur at the same potential. In **2** (as well as in its stereochemically pure isomers, see later), simultaneous one-electron oxidations of each metal occur (Table 2), suggesting negligible electronic

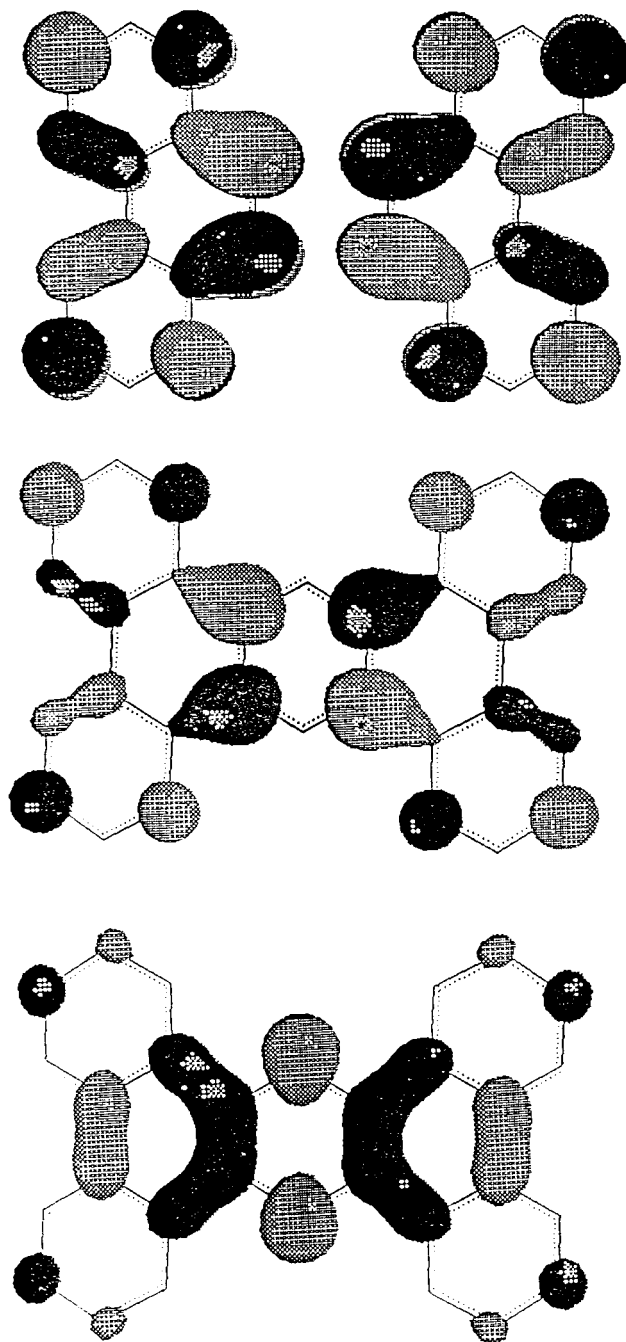


Figure 6. LUMO and LUMO+1 for tpphz and LUMO of phenanthroline as determined by ab initio calculations using the 3-21G basis set. HOMO's (not shown) -8.19 eV (tpphz) and -8.33 eV (phen).

interaction between the metals. This behavior is similar to that reported for the complex $[(bpy)_2Ru(\mu\text{-tpphz})Ru(bpy)_2]^{4+}$.²⁰ It should be considered, anyway, that this does not mean there is no interaction between the chromophores, neither that interchromophore processes are not allowed. Interchromophore electronic interaction as small as few cm^{-1} , negligible by an electrochemical viewpoint, can drive fast electron and/or energy transfer processes.^{1a} The negligible metal–metal interaction observed in **2** was unexpected due to the planar, conjugated structure of the bridging ligand, however, it can be explained on taking into account the superexchange mechanism mediating metal–metal interaction.^{21,23} The electron-transfer pathway of such a mechanism, that is the effective pathway for superexchange in the case of bridging ligands with low-lying π^* orbitals,²¹ depends on the electronic coupling between $d\pi$ metal

(21) Giuffrida, G.; Campagna, S. *Coord. Chem. Rev.* **1994**, *135–136*, 517 and references therein.

(22) Ward, M. D. *Chem. Soc. Rev.* **1995**, 121.

orbitals and the π^* orbitals of the bridge and on a "conduction pathway" within the bridge (the way the two chelating sites of the bridge are connected one another).²¹ Most likely the LUMO orbital of tpphz is hardly involved in the superexchange mechanism because of its very low coupling with the $d\pi$ metal orbitals (it receives negligible contribution from the phenanthroline nitrogens which interact with the metals, as discussed before), and LUMO+1, although having strong electronic coupling with $d\pi$ metal orbitals, has a less efficient "conduction pathway" (there is a little communication between the two chelating sites, because this orbital has negligible contribution from the central pyrazine ring which behaves as an isolating spacer as far as the chelating sites of tpphz are concerned). The constancy of the potential of the metal oxidation on passing from **1** to **2** further indicates that second metalation does not significantly modify the energy level of tpphz LUMO+1 orbital. In fact, significant changes of LUMO+1 orbital energy should influence metal oxidation potential by modifying the interaction between $d\pi$ metal orbital and LUMO+1.

In the dendritic complex **4** (as well as in its stereochemically pure isomers), the central Ru metal experiences a different chemical environment from the three peripheral subunits (three tpphz ligands for the former compared to one tpphz and two phen ligands for the latter ones). Because tpphz is a better electron withdrawing ligand than phen, oxidation of the central subunit is expected to occur at more positive potential than oxidation of the three peripheral subunits. Cyclic voltammetry and DPV indeed confirm this expectation, showing a three-electron process, assigned to simultaneous one-electron oxidation of the three noninteracting peripheral metal subunits, followed by a one-electron process corresponding to oxidation of the central metal. The situation is qualitatively similar to that found in acetonitrile for other dendritic tetranuclear Ru systems based on 2,3-bis(2'-pyridyl)pyrazine as the bridging ligand.^{4c,5a,24} However, in that case oxidation of the central Ru(II) metal was not seen, because the interaction between the (oxidized) peripheral Ru centers and the central metal was much stronger and the oxidation of the inner metal was displaced out of the potential window usually available. To the best of our knowledge, **4** is the first dendritic species containing nonidentical Ru(II) centers as branching sites in which oxidation of inner metals occurs within the acetonitrile potential window. The reason for such a behavior is the negligible interaction, from an electrochemical viewpoint, between peripheral and central redox-active centers across the tpphz bridge. Very recently, oxidations of inner metals of dendrimers based on 2,3-bis(2'-pyridyl)pyrazine bridging ligands have been reported in liquid SO₂ at very positive potentials.²⁵ Inner Ru (II) oxidations in acetonitrile have been previously reported for dendrimers based on terpy-derivative bridging ligands,^{6b} but in those cases the chemical environment of peripheral and inner metals are practically identical.

By comparison with the redox data of the mononuclear compounds (Table 2), the reduction pattern of **2** suggests that the first reduction involves the pyrazine-centered LUMO orbital of tpphz. The second and third processes are bielectronic, and

involve simultaneous one-electron reduction of two phen linked to different metals, followed by simultaneous reduction of the other two not yet reduced phen. According to the behavior of the mononuclear complex **1**, the reduction of LUMO+1 of tpphz is displaced to more negative potentials because of the prior reduction of the pyrazine fragment, so that second reduction of the bridge, centered on LUMO+1, does not occur within the reduction potential window investigated. Also in this case, the results agree with the reduction pattern of [(bpy)₂Ru(*u*-tpphz)-Ru(bpy)₂]⁴⁺.²⁰ It is interesting to note that the reduction potential of tpphz LUMO shifts to less negative values on passing from **1** to **2**, suggesting that the energy level of the pyrazine-centered orbital of the bridge is lowered upon second metalation.

The dendritic complex **4** exhibits two successive three-electron reduction processes (Table 2) followed by other multielectron processes whose number of electrons is difficult to determine because of adsorption problems. By comparison with the reduction pattern of **2**, the first process is assigned to simultaneous one-electron reductions of the pyrazine sites on the three tpphz ligands, and the second process is attributed to reduction of three peripheral phen ligands linked to different metals. The absence of sizable interaction between the pyrazine sites of the tpphz ligands (i.e.; tpphz-LUMO orbitals) linked to the same (central) metal, is demonstrated by their simultaneous reduction and confirms that little electronic interaction occurs between the tpphz LUMO and metal $d\pi$ orbitals.

Absorption Spectra. The absorption spectra of all the complexes studied here are straightforward. The absorption bands in the visible (Table 1, Figures 3 and 4) can be safely assigned to spin-allowed MLCT transitions, whereas the absorption bands in the UV are assigned to LC transitions. Such assignments are based on the energies and intensities of the bands when compared to other MLCT and LC bands of Ru(II) polypyridine complexes.¹⁷ In particular, the two absorption peaks in the region 350–400 nm which are present in the compounds containing tpphz can be assigned to transitions centered on this ligand (such peaks are, in fact, absent in the spectra of compounds **A–C**), in agreement with what reported for other tpphz-containing Ru(II) complexes.^{20,26} The MLCT bands comprise several different transitions, also owing to the heteroleptic nature of most of the complexes, so that a detailed discussion of the contributions to this band is prevented. However, on considering the usual correlation between electronic spectroscopy and electrochemistry in Ru(II) polypyridine complexes,^{17,27,28} based on the validity of Koopmans theorem and the usual coincidence of the orbitals involved in the redox properties with the orbitals involved in the MLCT transitions, one could expect relatively large differences in the energies of the MLCT bands of several compounds. For example, the complexes containing phendione ligands could be expected to exhibit some MLCT transition at significantly lower energy than the usual Ru→phen CT; however, the absorption spectra of the corresponding complexes do not show (Figure 3) any feature at energy lower than 500 nm. This indicates that the correlation spectroscopy/electrochemistry does not hold for the dione-containing complexes, probably because the lowest energy Ru→phendione CT transitions have negligible oscillator strengths. A similar result is obtained for the complexes containing tpphz. For example, for **1** two different Ru→tpphz CT transitions at low energy are

- (23) (a) McConnell, H. M. *J. Chem. Phys.* **1961**, *35*, 508. (b) Miller, J. R.; Beitz, J. V. *J. Chem. Phys.* **1981**, *74*, 6746. (c) Richardson, D. E.; Taube, H. *J. Am. Chem. Soc.* **1983**, *105*, 40. (d) Newton, M. D. *Chem. Rev.* **1991**, *91*, 767. (e) Jordan, K. D.; Paddon-Row, M. N. *Chem. Rev.* **1992**, *92*, 395. (f) Todd, M. D.; Nitzan, A.; Ratner, M. A. *J. Phys. Chem.* **1993**, *97*, 29.
- (24) Denti, G.; Campagna, S.; Sabatino, L.; Serroni, S.; Ciano, M.; Balzani, V. *Inorg. Chem.* **1990**, *29*, 4750.
- (25) Ceroni, P.; Paolucci, F.; Paradisi, C.; Juris, A.; Roffia, S.; Serroni, S.; Campagna, S.; Bard, A. J. *J. Am. Chem. Soc.* **1998**, *120*, 5480.

- (26) Kelch, S.; Rehahan, M. *Macromolecules* **1997**, *30*, 6185.

- (27) (a) Ohsawa, Y.; Hanck, K. W.; De Armond, M. K. *J. Electroanal. Chem.* **1984**, *175*, 229. (b) Dodsworth, E.; Lever, A. B. P. *Chem. Phys. Lett.* **1985**, *119*, 61. (c) Curtis, J. C.; Sullivan B. P.; Meyer, T. J. *Inorg. Chem.* **1983**, *22*, 224.

- (28) Meyer, T. J. *Pure Appl. Chem.* **1986**, *58*, 1193.

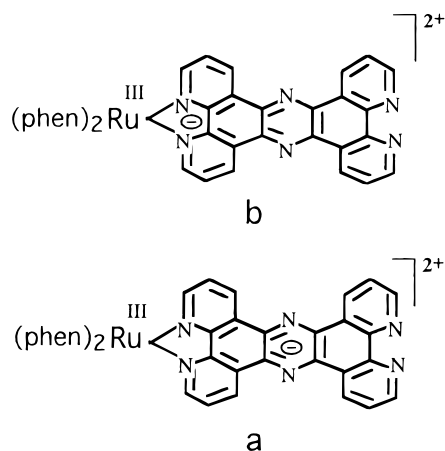


Figure 7. Representation of MLCT₀ (a) and MLCT₁ (b) excited states in tpphz-containing complexes (see text).

possible. One involves the pyrazine-centered LUMO as the acceptor orbital (Ru→tpphz(LUMO), herein after MLCT₀) and the other one (Ru→tpphz(LUMO+1), herein after MLCT₁) involves the phenanthroline-centered orbital of tpphz. The situation is shown schematically in Figure 7. The donor orbital of both transitions is mainly centered on the metal, so that the probability of the MLCT₁ transition is much larger than the probability of MLCT₀, because of the different electronic coupling between donor and acceptor orbitals. As a consequence, the MLCT₀ band is obscured in the absorption spectrum of **1** by the more intense MLCT₁ band. The same is also valid for the absorption spectra of all the higher-nuclearity tpphz-containing complexes studied here.

Within the tpphz-series of complexes, the extinction coefficient throughout all the UV and visible region increases with the number of the metal-based chromophores, while the profiles of the absorption spectra are quite similar (Table 1, Figure 4). This demonstrates that each chromophore contributes with its own properties to the overall absorption and that cross section with solar energy increases with the number of chromophores, as usual in multimetallic systems featuring little interaction between subunits.^{1d} Finally, comparison between the spectra of **1** and **2** indicate that the relative intensity of the LC absorption bands in the 350–400 nm region (i.e., the tpphz-centered transitions, see above) with respect to the MLCT bands (i.e., the visible region) decreases on passing from **1** to **2**. This agrees with the expectations based on the considerations given above, because on passing from **1** to **2** the number of MLCT transitions increases while the number of tpphz-centered transitions is maintained constant. It could be noted that tpphz should be modified in a different way by mono or di coordination. For example, tpphz is symmetric in **2**, whereas it is not symmetric in **1**. This could produce different effects on its electronic properties. Such effects are not discussed here because they are out of the aim of this work.

Photophysical properties. Mononuclear Precursors. For simplicity reasons, we will start the discussion on the luminescence properties of the precursor complexes with the 77 K results (Table 1, Figure 3). Emission of **C** can be easily assigned to the triplet MLCT state involving the derivatized phen ligand, because this compound is a homoleptic species. Then, one can note (Table 1) that the emission energy for **A** is very close to that of **C**, so we propose that also in this case the emission should be the same origin. For **B**, the lower emission energy compared with that of [Ru(phen)₃]²⁺ (Table 1) suggests that also in this case emission originates from ³MLCT involving

the derivatized ligand. Luminescence lifetimes, typical of ³MLCT emission in Ru(II) polypyridine complexes in glasses,^{17,28} further support the assignments.

The same ³MLCT assignments hold for the precursor complexes in fluid solution at room temperature, however, under such conditions **C** is not luminescent and **A** emits only very weakly (Table 1). The absence of room-temperature emission (or the reduced emission) for Ru(II) complexes containing dione groups has been reported in the literature.²⁹ In these complexes, the excited state responsible for luminescence is a MLCT state associated with a transition in which the acceptor orbital is mainly centered on the nitrogen of the polypyridine ligand; at room temperature in fluid solution, such a state can undergo oxidative electron-transfer involving an orbital centered on the dione moiety. The charge-separated species so formed undergoes fast radiationless decay to the ground state and as a consequence quenching of MLCT luminescence occurs. We propose this mechanism also occurs in **A** and in **C**.

Tpphz-Containing Complexes. As already discussed above, two low-lying MLCT states involving tpphz are present in **1**, both lower than Ru→phen CT excited state. On the basis of the redox properties, the lowest excited state should be the ³-MLCT₀ level, which lies at significantly lower energy than Ru→phen CT level. However, the energy ordering of MLCT₀ and MLCT₁ is difficult to state because of the different Coulombic stabilizations, due to the electron–hole attraction, expected for the two excited states. Luminescence of **1** occurs at an energy only slightly lower than that of [Ru(phen)₃]²⁺ (Table 1) both at room temperature in fluid solution and at 77 K in rigid matrix, so it is assigned in both cases to the triplet MLCT₁ state. Assignment to Ru→phen CT level was ruled out because such a state in **1** should lie at higher energy than MLCT₁ level and also at a higher energy than Ru→phen CT in [Ru(phen)₃]²⁺, because oxidation of the metal is more difficult in **1** than in [Ru(phen)₃]²⁺. Similar assignment has been proposed for other Ru(II) complexes containing tpphz²⁰ and the closely related ligand phehat (phehat = 1,10-phenanthroline[5,6-*b*]1,4,5,8,9,12-hexaazatriphenylene).³⁰ The larger luminescence quantum yield and longer lifetime at room temperature of **1** compared to [Ru(phen)₃]²⁺ (Table 1) are probably related to an increased energy gap between the luminescent level and the closely lying ³MC excited state, which is known to deactivate ³MLCT levels of Ru(II) polypyridine complexes by thermally activated surface crossing.^{17,28} The energy of the ³MC state is most likely similar or slightly higher in **1** compared to [Ru(phen)₃]²⁺, because it depends to a large extent from the arrangements of the ligands around the metal in the octahedral geometry, whereas the emitting MLCT level decreases in energy. The ³MC state cannot play any role at 77 K, where [Ru(phen)₃]²⁺ exhibits a longer lifetime.

The following arguments can be considered to rationalize the luminescence properties. The excited-state populated by direct excitation in **1** is MLCT₁ (spin is not considered here for simplicity). In principle, such a state could deactivate to the MLCT₀ level. According to Figure 7, the conversion from MLCT₁ to MLCT₀ can be viewed as a deactivation between excited states or, in a “supramolecular/multicomponent approach”, as an oxidative electron transfer from the Ru→tpphz (LUMO+1) CT state to the “covalently-linked” pyrazine, with production of the Ru→tpphz(LUMO) CT level. When the

(29) Goulle, V.; Harriman, A.; Lehn, J.-M. *J. Chem. Soc., Chem. Commun.* **1993**, 1034.

(30) Moucheron, C.; Kirsch-De Mesmaeker, A.; Choua, S. *Inorg. Chem.* **1997**, *36*, 584.

second approach is considered, the driving force ΔG for the process can be calculated in a first approximation by eq 1 (neglecting the entropy factor and the work term).³¹

$$\Delta G = e[E_{\text{ox}}^* - E_{\text{red}}] \quad (1)$$

In this equation, e is the electron charge, E_{ox}^* is the oxidation potential of the excited state, $E_{\text{ox}}^* = E_{\text{ox}} - E_{00}$, where E_{ox} is the oxidation potential of the ground state and E_{00} is the excited-state energy, approximated by the 77 K emission maximum, and E_{red} is the reduction potential of the pyrazine-centered acceptor (taken as the first reduction potential of the **1**). By introducing the experimental data (Tables 1 and 2) in eq 1, a value of +0.2 eV is obtained. The electron-transfer process leading to deactivation of MLCT₁ and population of MLCT₀ is therefore an endoenergetic process, so that its rate constant can be relatively slow because of the intrinsic nuclear barrier for the electron transfer, and could not compete with the deactivation of MLCT₁ to the ground state. The results, according to the experiments, is that the luminescence properties of **1** are governed by MLCT₁.

Looking at the luminescence data in Table 1 and to Figure 5, it appears that the luminescence spectra and lifetimes of **2** are close to those of **1** at 77 K, whereas they are quite different at room temperature. This suggests different origins for luminescence of **2** under different conditions. If the relevant data obtained for **2** (Tables 1 and 2) are now inserted into eq 1, the driving force for the electron-transfer producing MLCT₀ from MLCT₁ is -0.01 eV. It should be noted that this implies a significant energy change in the LUMO or LUMO+1 (or both) upon double coordination (we postulate that the LUMO+1 is raised in energy relative to the LUMO because the additional metal d- π^* overlap is expected to destabilize the LUMO+1 more than the LUMO. While the redox data suggests a lowering of the LUMO upon going from mono to double coordination, the lowered reduction potential may be anticipated on purely Coulombic arguments considering the central position of the bridging ligand and the increased charge. Furthermore, owing to the uncertainties in the experimental data and the approximations used (which include neglect of the outer reorganizational energy upon the electron transfer), the calculated ΔG values for the electron transfer processes are most likely not exact; this does not affect the discussion because the driving force for the MLCT₁→MLCT₀ conversion surely increases on passing from **1** to the oligonuclear systems, also when experimental uncertainties are taken into account). A driving force for electron-transfer equivalent to -0.01 eV can lead to a fast MLCT₁→MLCT₀ process in fluid solution at room temperature, but it cannot drive the above cited deactivation process in rigid matrix at 77 K. The situation is schematized in Figure 8. Emission of **2** is therefore assigned to MLCT₀ at room temperature and to MLCT₁ at 77 K. It can be noted that, according to such a view, MLCT₀ can be viewed as a luminescent charge-separated state, similar to the one reported for a Ru(II) complex containing the electron acceptor 1-methyl-4,4'-bipyridinium cation.³² The shorter luminescence lifetime and reduced quantum yield of **2** compared to **1** can be attributed to enhanced rate constant of the radiationless transitions due to the energy gap law^{17,28} and/or modification in the nature of the

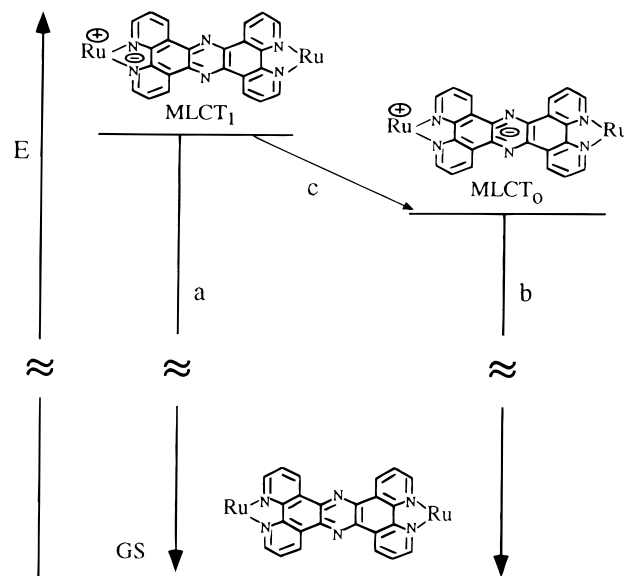


Figure 8. Energy level diagram and deactivation processes for the lowest-lying excited states in dinuclear complexes. For the sake of simplicity, peripheral ligands, charges of complexes, and spin multiplicity are neglected. Processes *a* and *b* are the direct deactivations from MLCT₁ and MLCT₀ to the ground state, respectively, and *c* is the energy transfer process interconverting the two excited states. Such a process, owing to its small driving force, is temperature dependent (see text).

luminescent CT level. The latter point can be significant, in that deactivation of MLCT states involving pyrazine moieties can be strongly assisted by the solvent.³³ The shorter intrinsic excited-state lifetime of MLCT₀ compared to that of MLCT₁ (i.e., the excited-state lifetime when deactivation to MLCT₀ does not take place, which can be inferred by the luminescence lifetime of **1**) can also induce irreversibility to the almost isoenergetic MLCT₁→MLCT₀ electron-transfer process occurring in **2**.

As for **4**, because of the presence of metals having $d\pi$ orbitals at different energies (see redox behavior), two different MLCT₁ ($\text{Ru}_{\text{peripheral}} \rightarrow \text{tpphz}(\text{LUMO}+1)$ CT and $\text{Ru}_{\text{central}} \rightarrow \text{tpphz}(\text{LUMO}+1)$ CT) and two different MLCT₀ ($\text{Ru}_{\text{peripheral}} \rightarrow \text{tpphz}(\text{LUMO})$ CT and $\text{Ru}_{\text{central}} \rightarrow \text{tpphz}(\text{LUMO})$ CT) transitions at different energies are present in **4**. In general, the $\text{Ru}_{\text{peripheral}} \rightarrow \text{tpphz}$ CT transition lies at lower energy than the corresponding $\text{Ru}_{\text{central}} \rightarrow \text{tpphz}$ CT one. The similarity of the absorption spectrum of **4** with that of **2** indicates that it is dominated by MLCT₁ transitions, and that MLCT₀ transitions do not contribute significantly to the visible bands, as also discussed before.

The emission at 77 K of **4** (Figure 5) is assigned to a triplet MLCT₁ state, on the basis of comparison between the photophysical properties of the other complexes studied here (Table 1). Furthermore, the shift of the emission toward lower energies compared to the emission of **2** suggests that the luminescent level involves the peripheral metals rather than the central chromophore. In fact, the MLCT₁ level involving the central metal would lie at higher energy, being the central metal in **4** more difficult to oxidize than the Ru(II) metals in **2**. Because the emission spectrum does not change on changing excitation wavelength, the MLCT₁ level involving the central metal does not directly contribute to the emission process and energy

(31) (a) *Photoinduced Electron Transfer*; Fox, M. A.; Chanon, M., Eds.; Elsevier: New York, 1988. (b) Scandola, F.; Indelli, M. T.; Chiorboli, C.; Bignozzi, C. A. *Top. Curr. Chem.* **1990**, *158*, 73. (32) Coe, B. J.; Friesen, D. A.; Thompson, D. W.; Meyer, T. J. *Inorg. Chem.* **1996**, *35*, 4575.

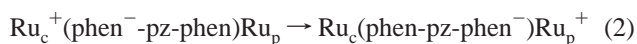
(33) (a) Amouyal, E.; Homsí, A.; Chambron, J. C.; Sauvage, J.-P. *J. Chem. Soc., Dalton Trans.* **1990**, 1841. (b) Friedman, A. E.; Chambron, J.-C.; Sauvage, J.-P.; Turro, N. J.; Burton, J. K. *J. Am. Chem. Soc.* **1990**, *112*, 4960. (c) Nair, R. B.; Cullum, B. M.; Murphy, C. J. *Inorg. Chem.* **1997**, *36*, 962.

transfer from $\text{Ru}_{\text{central}} \rightarrow \text{tpphz}(\text{LUMO}+1)$ CT excited state to $\text{Ru}_{\text{peripheral}} \rightarrow \text{tpphz}(\text{LUMO}+1)$ CT takes place. At room temperature in fluid solution, luminescence spectrum, lifetime, and quantum yield suggest that emission originates from a triplet MLCT_0 , also involving a peripheral metal. Even under these conditions, the emission spectrum does not change on changing excitation wavelength, so that direct emission from the higher-lying MLCT_0 state most likely does not contribute to the overall emission process. Anyway, emission originating from thermally equilibrated states cannot be excluded in this case.

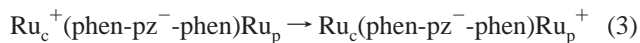
The same arguments employed to explain the different origin of the emission at room temperature and at 77 K in **2** can be used for **4**, being the driving force for the $\text{MLCT}_1 \rightarrow \text{MLCT}_0$ interconversion in **4** equivalent to +0.04 eV from eq 1. It should be noted that the room-temperature luminescence observed in **4** is at higher energy than that observed in any other luminescent dendritic multimetallic species reported so far (compare, for example, the room-temperature emission maxima of **4** given in Table 1 with the emission maxima of $[\text{Ru}\{\mu\text{-}2,3\text{-dpp}\}\text{Ru}\{\mu\text{-}2,3\text{-dpp}\}\text{Ru}(\text{bpy})_2\}_3]^{20+}$, that is about 810 nm; 2,3-dpp = 2,3-bis-(2-pyridyl)pyrazine).^{4c} This suggests that the systems studied here can store a higher energy and ultimately may be able to drive more endothermic processes.

The matching between absorption and excitation spectra of **4** at room temperature indicates that the light absorbed by all the chromophores is quantitatively transferred to the emission state, so we can conclude that in **4** energy transfer from the (higher-lying) central chromophore to the (lower-lying) peripheral ones takes place with high efficiency. Although reliable excitation spectra were not obtained at 77 K because of technical problems, the monoexponential decay and the constancy of the emission spectra on changing excitation wavelength suggests that the process is also effective under such conditions.

Some considerations concerning the energy transfer process mechanism at room temperature and at 77 K can be made. At 77 K, the energy transfer process most likely occurs between MLCT_1 excited states. It can be schematized as in eq 2, in which tpphz is represented as phen-pz-phen to emphasize the segmented excited-state properties of the two phenanthroline-like chelating sites and the pyrazine central moiety, and central and peripheral metals are labeled as Ru_c and Ru_p , respectively (only a branch of the dendrimer is represented for simplicity).



The process is a real energy transfer in that double electron exchange is required. At room temperature in fluid solution, the energy transfer would involve MLCT_0 levels, so that the energy transfer process can be schematized as in eq 3.



In this case, the energy transfer process could be essentially considered as a single electron-transfer process. In the case of **4**, different mechanisms for the energy transfer could therefore be effective on changing temperature and medium rigidity. Anyway, the boundaries between energy and electron-transfer processes in polynuclear metal complexes are indeed ambiguous in many cases.^{1d,34} For example, it should be also considered that in a more rigorous description, charge distribution of the

unpaired electron on the pyrazine moiety should change upon the electron-transfer represented by eq 3, so that also this process could be considered as an electron-exchange energy transfer.

Photophysical and Redox Properties of the Stereoisomers.

The effect of stereoisomerism on photophysical properties of polynuclear metal complexes is a topic only recently addressed. It is of a large interest because of the consequences that could have for the construction of very large metal-based supramolecular architectures exhibiting charge separation and energy migration functions, as well as for interaction of these systems with chiral substrates such as biological ones. From the data reported in Tables 1 and 2 and taking into account the experimental uncertainties, it can be noticed that the absorption spectra, the luminescence properties, and the redox behavior of the various stereoisomers studied here are practically undistinguishable one another and are identical to those of the racemic species. In the stereochemically pure tetranuclear dendrimers, the energy transfer process from the central chromophore to the peripheral ones is quantitative, so that it is not possible to compare the efficiencies of the processes for the various diastereoisomers.

While the absence of a sizable effect of chirality on the spectroscopic and redox properties was indeed expected for enantiomers, it was not obvious for diastereoisomers. Identical photophysical and redox properties for diastereoisomers of other trinuclear Ru(II) complexes have been reported,¹³ whereas significant differences were found as far as the luminescence lifetimes at 77 K are concerned for different diastereoisomers of polynuclear Ru(II) complexes based on the bridging ligand HAT (HAT = 1,4,5,8,9,12-hexaazatriphenylene).¹² In particular, in the latter systems shorter luminescence lifetimes were found at 77 K for stereoisomers in which subunits having different chirality were contemporary present. No interpretation of these results, anyway, was proposed.

It could be noted that in the systems in which an effect of the stereoisomerism on photophysical properties was found,¹² a noticeable interaction between the chromophores was reported. On the contrary, in the systems studied here and in the polynuclear complexes reported in the literature¹³ in which stereoisomerism seems to have negligible effects on absorption and luminescence properties, only weak interactions between the chromophores takes place. However, a more detailed discussion of our results in comparison with other literature data is speculative in the absence of a more examples.

Conclusions

The absorption spectra, luminescence properties, and redox behavior of stereochemically pure dendritic Ru(II) tetramers have been studied. Furthermore, the investigation has also been performed on stereochemically resolved dinuclear complexes of the same family and on racemic forms of their mononuclear precursors and models. The results show that the fully conjugated bridging ligand used to assemble the configurationally pure dendrimers and dinuclear complexes confers peculiar properties. The metal-metal electronic interaction across such a bridge is electrochemically not sizable. However, intercomponent energy transfer leading to the excitation of the component(s) in which the lowest energy state(s) is (are) located occurs in the dendritic species. Luminescence originates from different MLCT states on changing the experimental conditions (i.e., temperature and medium rigidity). The diastereoisomers exhibit spectroscopic, photophysical, and redox properties which do not depend on the stereochemical arrangements of the multinuclear array, when experimental uncertainties are taken into account.

(34) (a) Juris, A.; Balzani, V.; Campagna, Denti, G.; Serroni, S.; Frei, G.; Güdel, H. U. *Inorg. Chem.* **1994**, *33*, 9086. (b) Serroni, S.; Campagna, S.; Denti, G.; Keyes, T.; Vos, J. G. *Inorg. Chem.* **1996**, *35*, 4513.

A comparison with the properties of other configurationally pure luminescent and redox-active multinuclear Ru(II) species has been attempted, but a detailed discussion of this topic is limited by the absence of a significant number of other systems.

Because of their spectroscopic, photophysical, and redox properties, the studied species are quite promising to play the role of configurationally pure antennae in larger systems. Owing to their optical purity and to the conformational rigidity of the overall structure, they are also of interest as chiral photocatalysts and luminescent sensors/probes for chiral systems.

We are at the present engaged in the synthesis of larger stereochemically pure Ru(II) dendrimers as well as of mixed-

metal systems containing tpphz and similar bridges for directional energy transfer to design more efficient light-harvesting systems and to study in further detail the effect of the chirality on the photoinduced intercomponent transfer processes.

Acknowledgment. We thank MURST (Progetto "Dispositivi Supramolecolari"), CNR, and the Robert A. Welch Foundation (Grant Y-1301) for financial support. We also thank Prof. Margherita Venturi for helpful discussions and Dr. Loredana Rubino for preliminary experiments.

IC9811852